

Rotational states of an adsorbed dipole molecule in an external electric field

Y. T. Shih*

*Graduate Institute of Opto-electronic Engineering, National Changhua University of Education, Changhua, Taiwan 50058, Republic of China*Y. Y. Liao and D. S. Chuu[†]*Institute of Electrophysics, National Chiao Tung University, Hsinchu, Taiwan 30050, Republic of China*

(Received 15 February 2002; revised manuscript received 3 March 2003; published 7 August 2003)

The rotational states of an adsorbed dipole molecule in an external electric field were investigated. The surface hindering potential was modeled as a finite conical well and a dipole-field interaction was added to the hindering potential. The molecular wave functions were expressed in terms of the eigenfunctions of molecular hindered rotation in the absence of electric field. Eigenenergies were determined by the matrix diagonalization procedures. Our results showed that, for both vertically and horizontally adsorbed molecules, there is avoided crossing between two adjacent rotational energy levels, as the field strength is increased, and finally all state energies decrease rapidly as the field strength is strong enough. The avoided crossing is due to the redistribution of wave function between different potential well regions. By employing the sudden unhindrance approximation, the rotational-state distributions of molecules desorbing from a solid surface in the presence of external electric field were calculated. Our results showed that the rotational-state distributions are significantly influenced by the external electric field. Since the electric field increases the ground-state energy of adsorbed molecule, the distribution shifts towards the high- J region if the electric field is applied to orient the molecular axis against the molecular preferred orientation. On the contrary, the distribution shifts towards the low- J region if the electric field is applied to orient the molecular axis towards molecular preferred orientation because the electric field decreases the ground-state energy of adsorbed molecule. The solutions to the finite conical well were also used to calculate the rotational alignment in the photodesorption of CO from Cr₂O₃(0001). Our results showed that at low- J values the CO molecules desorb like a helicopter, while at high- J values a cartwheel-like motion is preferred. This result is in qualitative agreement with the experimental observation.

DOI: 10.1103/PhysRevB.68.075402

PACS number(s): 73.20.Hb, 33.55.Be, 33.20.Sn

I. INTRODUCTION

The rotational motion of a molecule that interacts with a solid surface has attracted increasing interest. Experimental and theoretical investigations of the rotational distribution of scattering or desorbing molecules have been an active research field.¹⁻¹⁸ The measured rotational-state distributions of molecules scattering or desorbing from surfaces were found to exhibit a substrate temperature-independent non-Boltzmann feature.¹⁻³ On the other hand, the theoretical studies on the rotational motion of adsorbed molecules have been also reported. Gadzuk and his co-workers⁴⁻⁷ proposed an infinite-conical-well model, in which the adsorbed molecule is only allowed to rotate within the well region, to mimic the surface hindering potential. Rotational-state energy spectra for both vertical and horizontal adsorption configurations were obtained. Together with the sudden unhindrance approximation, the non-Boltzmann property of the rotational-state distributions can be attributed to the hindered rotations of adsorbed molecules. In our previous works,⁸⁻¹⁰ we proposed a finite-conical-well model to generalize the study of a finite hindrance. Our results showed that the rotational-state distributions of desorbing molecules are non-Boltzmann and display oscillatory structures with alternate drops and plateaus. A similar structure was observed in a gas-surface scattering experiment and was interpreted in terms of rotational rainbows.¹⁹ The oscillatory structure ob-

tained in our previous studies is a general result of a system transiting from hindered states to free states, and can be regarded as the manifestation of the rotational invariance. Our calculated results have been found in good agreement with the previously measured data.³

The surface physics and chemistry in high electric fields have attracted great interest since the inventions of field emission microscope (FEM)²⁰ and field ion microscope (FIM).²¹ In these microscopes, a strong electric field of the order of 1 V/Å is applied to the tip of a sharp metal wire. In such high electric field, many effects can occur. For example, the tunneling through a field-deformed barrier at the surface of the metal is possible. This is responsible for the field emission, field ionization, and field desorption/evaporation processes.^{22,23} On the other hand, in a strong electric field of the order of 10⁻¹ V/Å, the electronic orbitals may be distorted so that the chemical characteristics of atoms or molecules are affected. Therefore, the chemical effects by establishing new bonding orbitals may occur. In this way, molecules that are unstable in field free situations may be stabilized by strong electric field. Also, new pathways of chemical reaction may be established.²⁴

It is well known that the rotational energy levels of a free molecule placed in an electric field are split due to the interaction between molecular dipole moment and electric field.²⁵ In addition to the splittings, theoretical investigation²⁶ showed that, when the applied electric field is strong, mo-

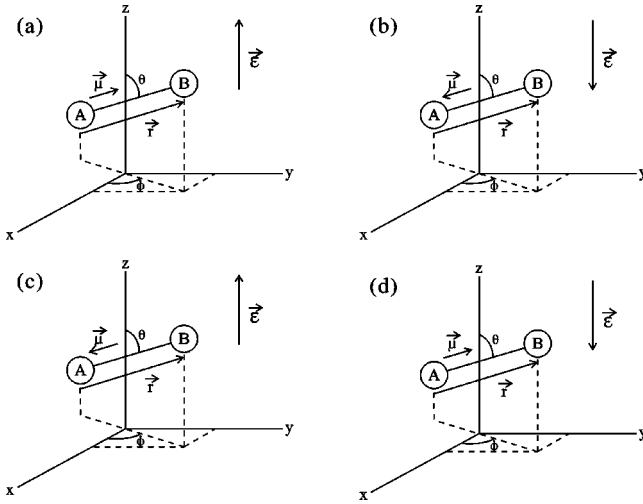


FIG. 1. An adsorbed diatomic molecule with a dipole moment $\vec{\mu}$ in the presence of perpendicular electric field $\vec{\epsilon}$.

molecular rotational energies have large negative shifts. On the other hand, in our previous work,⁹ we have investigated the external electric field effect on the ground-rotational-state energy of an adsorbed dipole molecule. We considered that an dipole-field interaction was added to the finite-conical-well potential. Our results showed that the Stark shift of ground-rotational-state energy will be suppressed by the conical-well potential if the field strength is smaller than the hindering potential. However, when the applied field is very strong, large Stark shift may take place.

In our previous investigation, the variational method was utilized and only the Stark shift of ground-state energy of horizontally adsorbed molecule was considered. In this work, we extended the investigation to the Stark shift of the excited rotational states for both cases of vertically and horizontally adsorbed molecules. Instead of using variational wave functions, the molecular wave functions we used in this work were expressed in terms of the eigenfunctions of molecular hindered rotation in the absence of electric field. Therefore, ground state and excited state energies can be determined simultaneously. One can see that the Stark shifts of rotational energies of adsorbed molecules show interesting behaviors. Besides, the rotational-state distributions of molecules desorbing from a solid surface in the presence of external electric field can be calculated. One can see the distributions are significantly influenced by the applied electric field.

II. MODEL AND FORMULISM

Figure 1 shows the situations that an adsorbed diatomic molecule with a dipole moment $\vec{\mu}$ in the presence of perpendicular electric field $\vec{\epsilon}$. The Hamiltonian of such system is

$$H = \frac{\hbar^2}{2I} L^2 + U^{\text{rot}}(\theta, \phi) - \mu \epsilon \cos \gamma, \quad (1)$$

where I is the molecular moment of inertia, $\hbar L$ is the angular momentum operator, γ is the angle between $\vec{\mu}$ and $\vec{\epsilon}$, and $U^{\text{rot}}(\theta, \phi)$ is the surface potential energy to which the molecule is subjected. As a first approximation we assume that $U^{\text{rot}}(\theta, \phi)$ is independent of ϕ . Calculation indicates that the dependence on ϕ is weaker than that on θ .²⁷⁻²⁹ We express the energy in the unit of the molecular rotational constant $B = \hbar^2/2I$; thus, Eq. (1) can be written as

$$H = L^2 + V^{\text{hin}}(\theta) - \omega \cos \theta, \quad (2)$$

where $V^{\text{hin}}(\theta)$ is the polar hindering potential energy to which the molecule is subjected. According to the finite-conical-well model,⁸⁻¹⁰ we assume

$$V^{\text{hin}}(\theta) = \begin{cases} 0, & 0 \leq \theta \leq \alpha \\ V_0, & \alpha < \theta \leq \pi, \end{cases} \quad (3)$$

for the vertical adsorption configuration, and

$$V^{\text{hin}}(\theta) = \begin{cases} 0, & \alpha \leq \theta \leq \beta \\ V_0, & 0 \leq \theta < \alpha \text{ or } \beta < \theta \leq \pi, \end{cases} \quad (4)$$

for the horizontal adsorption configuration. The parameter ω in Eq. (2) presents the strength of the dipole-field interaction:

$$\omega = \begin{cases} +\mu \epsilon / B, & \gamma = \theta \\ -\mu \epsilon / B, & \gamma = \pi - \theta. \end{cases} \quad (5)$$

The positive sign is for the cases of Figs. 1(a) and 1(b), while the negative sign is for the cases of Figs. 1(c) and 1(d). Therefore, $\omega > 0$ means the electric field orients the molecular axis toward molecular preferred orientation, while $\omega < 0$ means the electric field orients the molecular axis against molecular preferred orientation.

For the case that the applied electric field is absent, the Hamiltonian of the system is

$$H_0 = L^2 + V^{\text{hin}}(\theta). \quad (6)$$

There are analytic eigenfunctions for this system:⁸⁻¹⁰

$$\Psi_{l,m}^{(0)}(\theta, \phi) = \Theta_{l,m}^{(0)}(\cos \theta) \frac{\exp(im\phi)}{\sqrt{2\pi}}, \quad m = 0, \pm 1, \pm 2, \dots, \quad (7)$$

where

$$\Theta_{l,m}^{(0)}(\xi) = \begin{cases} C_{I,l,m} \mathcal{P}_{(+1)}(\nu_{l,m}, m, \xi), & \cos \alpha < \xi \leq 1 \\ C_{II,l,m} \mathcal{P}_{(-1)}(\nu'_{l,m}, m, \xi), & -1 \leq \xi < \cos \alpha, \end{cases} \quad (8)$$

for vertical adsorption configuration, and

$$\Theta_{l,m}^{(0)}(\xi) = \begin{cases} C_{I,l,m} \mathcal{P}_{(+1)}(\nu'_{l,m}, m, \xi), & \cos \alpha < \xi \leq 1 \\ C_{II,l,m} \mathcal{P}_{(+1)}(\nu_{l,m}, m, \xi) + D_{II,v,m} \mathcal{Q}_{(+1)}(\nu_{l,m}, m, \xi), & \cos \beta \leq \xi \leq \cos \alpha \\ C_{III,l,m} \mathcal{P}_{(-1)}(\nu'_{l,m}, m, \xi), & -1 \leq \xi < \cos \beta, \end{cases} \quad (9)$$

for horizontal adsorption configuration. The functions $\mathcal{P}_{(\pm 1)}$ and $\mathcal{Q}_{(+1)}$ in the above equations are defined as

$$\mathcal{P}_{(\pm 1)}(\nu_{l,m}, m, \xi) = (1 - \xi^2)^{|m|/2} F\left(|m| - \nu_{l,m}, 1 + |m| + \nu_{l,m}, 1 + |m|; \frac{1 \mp \xi}{2}\right), \quad (10)$$

$$\begin{aligned} \mathcal{Q}_{(+1)}(\nu'_{l,m}, m, \xi) &= (1 - \xi^2)^{|m|/2} \left\{ F\left(|m| - \nu'_{l,m}, 1 + |m| + \nu'_{l,m}, 1 + |m|; \frac{1 - \xi}{2}\right) \ln\left(\frac{1 - \xi}{2}\right) \right. \\ &+ \sum_{n=1}^{\infty} \frac{(|m| - \nu'_{l,m})_n (1 + |m| + \nu'_{l,m})_n}{(1 + |m|)_n n!} \left(\frac{1 - \xi}{2}\right)^n \\ &\times [\psi(|m| - \nu'_{l,m} + n) - \psi(|m| - \nu'_{l,m}) + \psi(1 + |m| + \nu'_{l,m} + n) - \psi(1 + |m| + \nu'_{l,m}) \\ &- \psi(1 + |m| + n) + \psi(1 + |m|) - \psi(1 + n) + \psi(1)] \\ &\left. - \sum_{n=1}^{|m|} \frac{(n-1)! (-|m|)_n}{(1 - |m| + \nu'_{l,m})_n (-|m| - \nu'_{l,m})_n} \left(\frac{1 - \xi}{2}\right)^{-n} \right\}, \quad (11) \end{aligned}$$

where $F(a, b, c; z)$ is the hypergeometric function.³⁰ In above equations, the molecular rotational energy has been expressed as

$$E_{l,m}^{(0)} = \nu_{l,m}(\nu_{l,m} + 1), \quad (12)$$

and $\nu'_{l,m}$ is defined as

$$\nu'_{l,m}(\nu'_{l,m} + 1) = \nu_{l,m}(\nu_{l,m} + 1) - V_0. \quad (13)$$

In order to determine $\nu_{l,m}$, one has to match the boundary conditions at $\xi_1 = \cos \alpha$ and $\xi_2 = \cos \beta$.

When the electric field is applied, there are no analytic eigenfunctions to the Hamiltonian, as shown in Eq. (2). However, consider that the system is still symmetric about z axis, we can express the eigenfunctions in terms of Eq. (7) for specific azimuthal quantum number m :

$$\Psi_m^{\text{hin}}(\theta, \phi) = \sum_{l'=m}^{\infty} c_{l',m} \Psi_{l',m}^{(0)}(\theta, \phi). \quad (14)$$

Substitute Eq. (14) into the Schrödinger wave equation, and multiply both sides of the equation by $\Psi_{l,m}^{(0)*}$ and then integrate it. We get

$$[E_{l,m}^{(0)} - E_m] c_{l,m} - \omega \sum_{l'} c_{l',m} \langle \Psi_{l,m}^{(0)} | \cos \theta | \Psi_{l',m}^{(0)} \rangle = 0. \quad (15)$$

The condition for nontrivial coefficients $c_{l',m}$ is, therefore,

$$\begin{vmatrix} E_{m,m}^{(0)} - E_m - \omega a_{m,m}^{m,m} & -\omega a_{m,m}^{m+1,m} & -\omega a_{m,m}^{m+2,m} & \dots \\ -\omega a_{m+1,m}^{m,m} & E_{m+1,m}^{(0)} - E_m - \omega a_{m+1,m}^{m+1,m} & -\omega a_{m+1,m}^{m+2,m} & \dots \\ -\omega a_{m+2,m}^{m,m} & -\omega a_{m+2,m}^{m+1,m} & E_{m+2,m}^{(0)} - E_m - \omega a_{m+2,m}^{m+2,m} & \dots \\ \vdots & \vdots & \vdots & \ddots \end{vmatrix} = 0, \quad (16)$$

where $a_{l',m}^{l',m} = \langle \Psi_{l',m}^{(0)} | \cos \theta | \Psi_{l',m}^{(0)} \rangle$. The eigenenergy E_m to Eq. (2) for specific azimuthal quantum number m can be obtained from solving this equation.

III. RESULTS AND DISCUSSION

A. Vertical adsorption configuration

For a vertically adsorbed molecule, the hindering potential energy can be modeled by Eq. (3). Figure 2 shows the

rotational-state energies of a vertically adsorbed dipole molecule in an external electric field as functions of field strength parameter $\omega > 0$ for azimuthal quantum number $m = 0$ and potential barrier heights $V_0 = 20$ and 80 . The hindrance angle is set as $\alpha = 30^\circ$. From Fig. 2, one can see that an applied electric field can induce shifts of adsorbed molecular rotational energies. When the electric field is increased, the ground-state energy decreases monotonously while the excited-state energies increase to a maximum and then decrease. The rate of the energy variation depends on

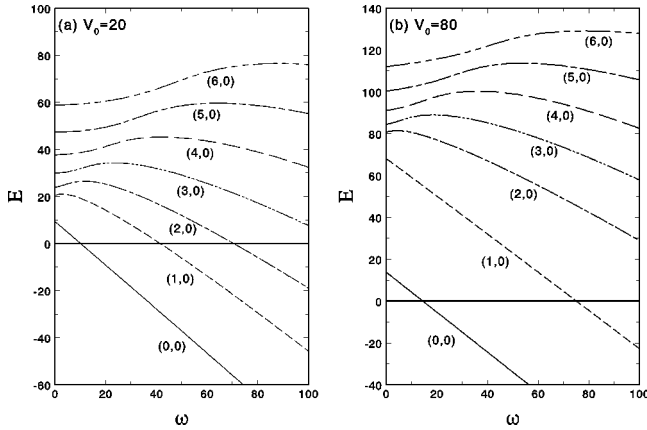


FIG. 2. Rotational-state energies of a vertically adsorbed dipole molecule in an external electric field as functions of field strength parameter $\omega > 0$ for azimuthal quantum number $m = 0$ and potential barrier heights $V_0 = 20$ and 80 . The hindrance angle is set as $\alpha = 30^\circ$.

the rotational state. The lower the state, the larger the rate. The behaviors of the rotational energies shown in Fig. 2 are similar to those of free dipole molecule in an electric field.²⁶ However, if the potential barrier is high enough, even the lower excited-state energies, e.g., the energy of $(1, 0)$ state of the $V_0 = 80$ case, show direct decreasing as the electric field is increased. This is different from that of a free dipole molecule.

Figure 3 shows the rotational-state energies of a vertically adsorbed dipole molecule in an external electric field as functions of field strength parameter $\omega < 0$ for azimuthal quantum number $m = 0$ and potential barrier heights $V_0 = 20$ and 80 . From Fig. 3 one can see that the variations of rotational energies for the case of $\omega < 0$ are very different from those for the case of $\omega > 0$. When the electric field is applied, the ground-state energy increases initially and then decreases as the field strength is stronger than some critical value. However, for the first excited $(1, 0)$ state of the V_0

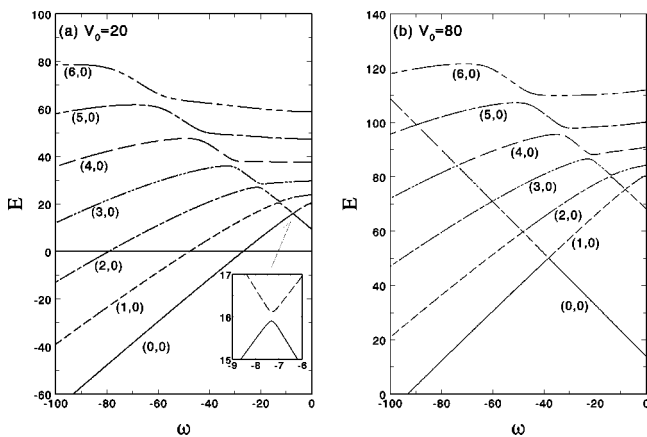


FIG. 3. Rotational-state energies of a vertically adsorbed dipole molecule in an external electric field as functions of field strength parameter $\omega < 0$ for azimuthal quantum number $m = 0$ and potential barrier heights $V_0 = 20$ and 80 . The hindrance angle is set as $\alpha = 30^\circ$.

$= 20$ case, the energy decreases initially and then increases to avoid the crossing of two energy levels at the same field strength. The avoided crossing between two levels also makes the ground-state energy to start to decrease at the same field strength. Finally, the energy of the $(1, 0)$ state decreases again for field strength stronger than another critical value. On the other hand, for the first excited $(1, 0)$ state of the $V_0 = 80$ case, the energy increases initially and then decreases at some critical field strength and then increases again to avoid crossing with the ground-state energy level. The avoided crossing also makes the ground-state energy to start to decrease at the same field strength. Finally, further decrease occurs for field strength stronger than another critical value. In Fig. 3, there are two or more avoided crossings for the other excited-state energies. The avoided crossing of two energy levels is a general result for the case of two very close levels with small perturbation where the Hamiltonian contains some parameter and its eigenvalues are consequently functions of that parameter.³¹

For the adsorbed molecule with higher potential barrier, there are more avoided crossings. Besides, for the adsorbed molecule with lower potential barrier height, their avoided crossings of higher energy levels become more smooth while compared with those with higher barrier height. Furthermore, the energies of two adjacent energy levels at the avoided crossing are very close to each other, especially for the lower states.

To analyze the variation of rotational energy with applied electric field, one may reexamine the potential energy for which an adsorbed molecule is subjected:

$$V(\theta) = V^{\text{hin}}(\theta) - \omega \cos \theta. \quad (17)$$

For the case of $\omega > 0$, when the external electric field is applied, the potential well is tilted to the $\theta = 0^\circ$ side and the potential energy $V(\theta)$ has a minimum at $\theta = 0^\circ$. That is, the electric field as well as conical well tend to concentrate molecular wave functions about $\theta = 0^\circ$. For the $(0, 0)$ state of the $V_0 = 20$ case or the $(0, 0)$ and $(1, 0)$ states of the $V_0 = 80$ case, since the vertical conical well confines the major part of molecular wave functions about $\theta = 0^\circ$ even the electric field is absent, an applied electric field will result in more concentration of the wave functions about $\theta = 0^\circ$ and then rotational energies are decreased rapidly. On the other hand, for other excited states, when the electric field is absent, the rotational energies are higher than the barrier height. Their wave functions are similar to those of free molecule and the major part of the wave functions distributes outside the conical well.⁸ An applied electric field will result in initially increasing the state energy. However, if the applied field is so large that molecular wave functions are forced to concentrate about $\theta = 0^\circ$, the rotational energies will decrease as the applied field is increased.

However, the case of $\omega < 0$ shows very different situation. Figures 4 and 5 show the potential energy $V(\theta)$ and the angular distributions of molecular wave functions $|\Psi|^2$ for a vertically adsorbed molecule as functions of θ for different electric field strengths. For comparison, the energy levels $E_{0,0}$ and $E_{1,0}$ are also indicated. From Figs. 4 and 5, one can

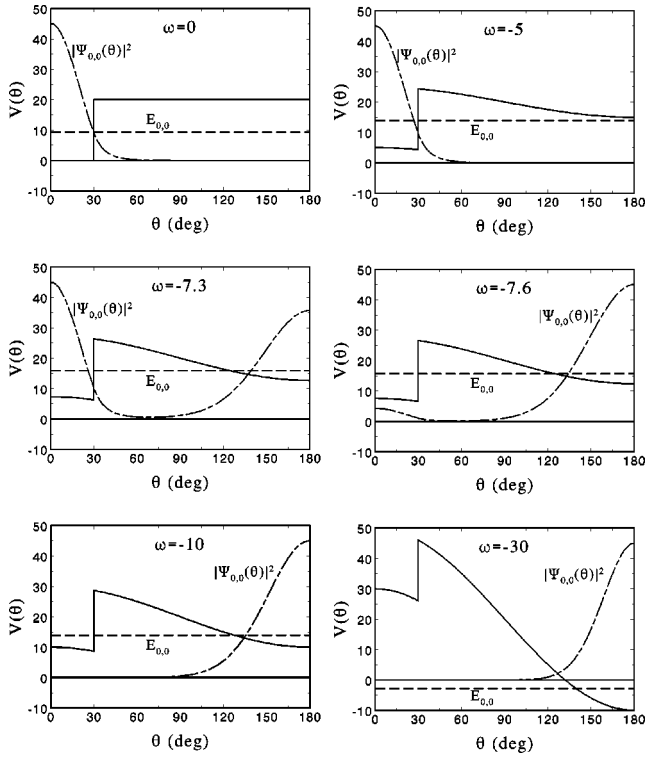


FIG. 4. Potential energy $V(\theta) = V^{\text{hin}}(\theta) - \omega \cos \theta$ and angular distribution of molecular wave function $|\Psi_{0,0}|^2$ for a vertically adsorbed molecule as functions of θ for different electric field strengths. $V^{\text{hin}}(\theta)$ is the vertical-conical-well hindering potential with $V_0 = 20$ and $\alpha = 30^\circ$.

see that, for the case of $\omega < 0$, the electric field not only tilts the conical potential well but also creates a new potential minimum at $\theta = 180^\circ$. That is, the applied electric field tends to turn over the vertically adsorbed molecule. Therefore, in fact, the problem treated in this work, for the polar space region $0^\circ \leq \theta \leq 180^\circ$, is equivalent to a double-well problem. This is absolutely different from the situation of a Cartesian square well subjected to an external electric field,^{32,33} and is the manifestation of the rotational invariance.

Employing Figs. 4 and 5, one can understand that the avoided crossing of two energy levels in Fig. 3 are due to the redistributions of molecular wave functions between two potential wells. For the ground-state, if the electric field is absent, the molecular wave function is confined initially in the $0^\circ \leq \theta < \alpha$ region by the vertical conical well. Therefore, the energy increases initially as the electric field is applied. However, when the electric field strength is increased up to the critical value so that $E_{0,0}$ is higher than the energy minimum about $\theta = 180^\circ$, it becomes energetically favorable to concentrate the wave function at $\theta = 180^\circ$. Hence the ground-state solution has now the character of the field-free (1, 0) state solution and its energy decreases as the applied field strength is increased.

On the other hand, for the excited (1, 0) state of the $V_0 = 20$ case, its energy decreases initially as an electric field is applied. However, when the ground-state wave function tunnels into the conical barrier region, the wave function of the

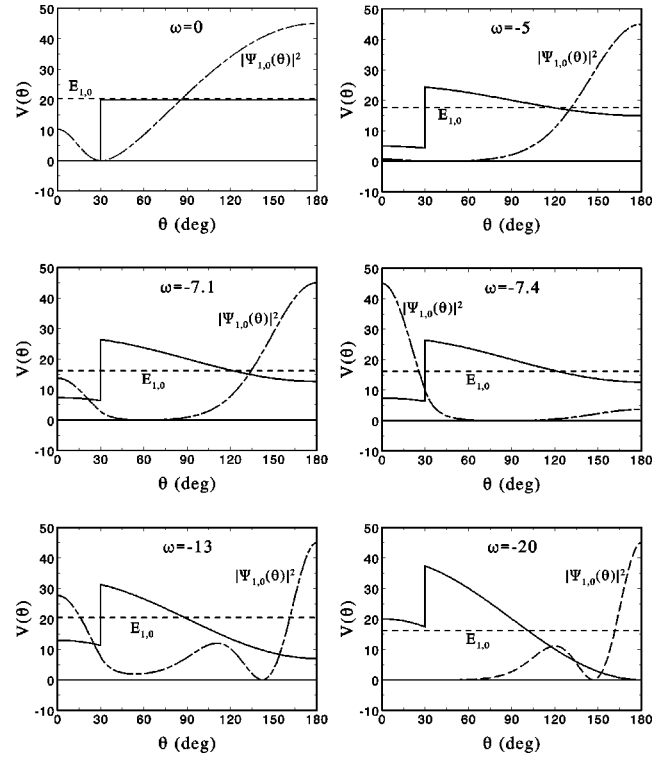


FIG. 5. Potential energy $V(\theta) = V^{\text{hin}}(\theta) - \omega \cos \theta$ and angular distribution of molecular wave function $|\Psi_{1,0}|^2$ for a vertically adsorbed molecule as functions of θ for different electric field strengths. $V^{\text{hin}}(\theta)$ is the vertical-conical-well hindering potential with $V_0 = 20$ and $\alpha = 30^\circ$.

excited (1, 0) state will tunnel into the conical well region to keep the orthogonality of wave functions. Hence it has now the character of the field-free ground-state solution and its energy increases as the applied field is increased. When the electric field strength is increased further to another critical value, the wave function of the (1, 0) state will tunnel back the region about $\theta = 180^\circ$ and then its energy decreases again. For the (1, 0) state of the $V_0 = 80$ case, when the electric field is absent, the wave function concentrates at $\theta = 0^\circ$ due to the higher potential barrier. Thus, as the field strength is increased, there is an additional energy change other than the (1, 0) state of the $V_0 = 20$ case. Similar discussions can be issued to other higher excited states. For larger field strengths more avoided crossings with the higher states occur. Beside, for the higher excited states whose energies are much higher than the potential barrier height, their wave function can smoothly redistribute over the polar space by an electric field. Thus their avoided crossings become smoother.

B. Horizontal adsorption configuration

For a horizontal adsorbed molecule, the hindering potential energy can be modeled by Eq. (4). Figure 6 shows the rotational-state energies of a horizontally adsorbed dipole molecule in an external electric field as functions of field strength parameter ω for azimuthal quantum number $m = 0$

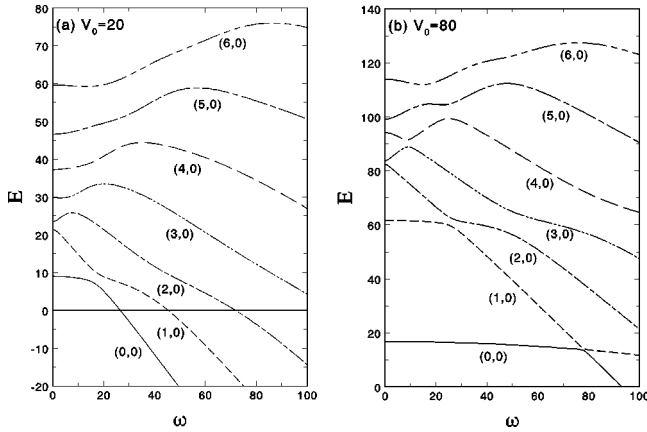


FIG. 6. Rotational-state energies of a horizontally adsorbed dipole molecule in an external electric field as functions of field strength parameter ω for azimuthal quantum number $m=0$ and potential barrier heights $V_0=20$ and 80 . The hindrance angle is set as $\alpha=75^\circ$ and $\beta=180^\circ-\alpha$.

and potential barrier heights $V_0=20$ and 80 . The hindrance angles are chosen as $\alpha=75^\circ$ and $\beta=180^\circ-\alpha$. Since the hindering potential is symmetric about the $\theta=90^\circ$ plane, the electric field effects on the rotational energies for $\omega>0$ case and $\omega<0$ case are the same. Therefore, we show the results for the $\omega>0$ case only. From Fig. 6, one can see that the ground-state energies of both $V_0=20$ and 80 cases decrease slowly as the electric field is applied and then rapid decrease occurs as the field strength is stronger than some critical value. However, the variation of excited-state energy is different. For $V_0=20$, the energy of $(1, 0)$ state decreases rapidly as the field is applied. When the state energy has decreased closely to the ground-state energy, the decrease rate becomes gentle to avoid the crossing of two energy levels. For further stronger electric field, the energy of the $(1,0)$ state decreases rapidly again. For the other excited states of the $V_0=20$ case, their energy variations shown in Fig. 6(a) are similar to those in Fig. 2(a).

On the other hand, for the $V_0=80$ case, the energy of $(1, 0)$ state decreases slowly and then rapidly. Finally, it decreases slowly again when the field strength is larger than the strength at which the energy of $(0, 0)$ state begins to decrease rapidly. For the other excited states of the $V_0=80$ case, the energy variations show in Fig. 6(b) are somewhat similar to those in Fig. 3. However, the avoided crossings are smoother and the gaps between two adjacent levels at these avoided crossings are larger than those in Fig. 3.

Figures 7 and 8 show the potential energy $V(\theta)$ and the angular distributions of molecular wave function $|\Psi|^2$ for a horizontally adsorbed molecule as functions of θ for different electric field strengths. The polar space is divided into three regions. When ω increases, the value of $V(\theta)$ decreases in region I ($0^\circ\leq\theta<\alpha$), and increases in region III ($\beta<\theta\leq 180^\circ$), but changes slightly in region II ($\alpha<\theta<\beta$).

For the ground $(0, 0)$ state, if the electric field is absent, molecular wave function is confined initially in the $\alpha<\theta$

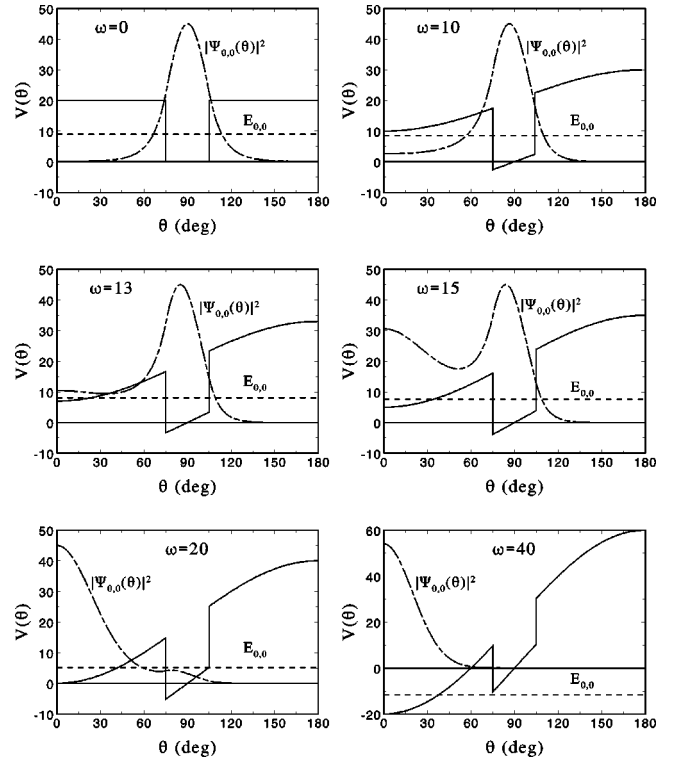


FIG. 7. Potential energy $V(\theta)=V^{\text{hin}}(\theta)-\omega\cos\theta$ and angular distribution of molecular wave function $|\Psi_{0,0}|^2$ for a horizontally adsorbed molecule as functions of θ for different electric field strengths. $V^{\text{hin}}(\theta)$ is the horizontal-conical-well hindering potential with $V_0=20$, $\alpha=75^\circ$, and $\beta=180^\circ-\alpha$.

$<\beta$ region by the vertical conical well. Therefore, the state energy varies gently as the field is applied, or one can say that the Stark shift of the rotational energy is suppressed by the conical well potential. However, when the electric field strength increases so that $E_{0,0}$ is higher than the energy minimum about $\theta=0^\circ$, the major part of the molecular wave function begins to distribute about $\theta=0^\circ$; therefore, the decrease of the state energy becomes rapid. When the electric field strength is very large, most of the molecular wave function will concentrate about $\theta=0^\circ$. This implies that the adsorption configuration changes from horizontal to vertical.

For the excited $(1, 0)$ state of the $V_0=20$ case, when the electric field is absent, the major part of the molecular wave function distributes in region I ($0^\circ\leq\theta<\alpha$) and region III ($\beta<\theta\leq 180^\circ$). When the electric field is applied, molecular wave function redistributes. The distribution in region I increases, and the distribution in region III decreases. Therefore, the energy decreases rapidly. If the applied electric field is further increased, considerable part of the wave function will concentrate in region II ($\alpha<\theta<\beta$), and the energy decreases slowly. When the electric field is so strong that most of the wave function concentrates in region I, the energy will decrease rapidly again. Similar discussions can be issued to other higher excited states. However, for those excited states whose rotational energies are much higher than the potential barrier height V_0 , the confinement potential is no longer

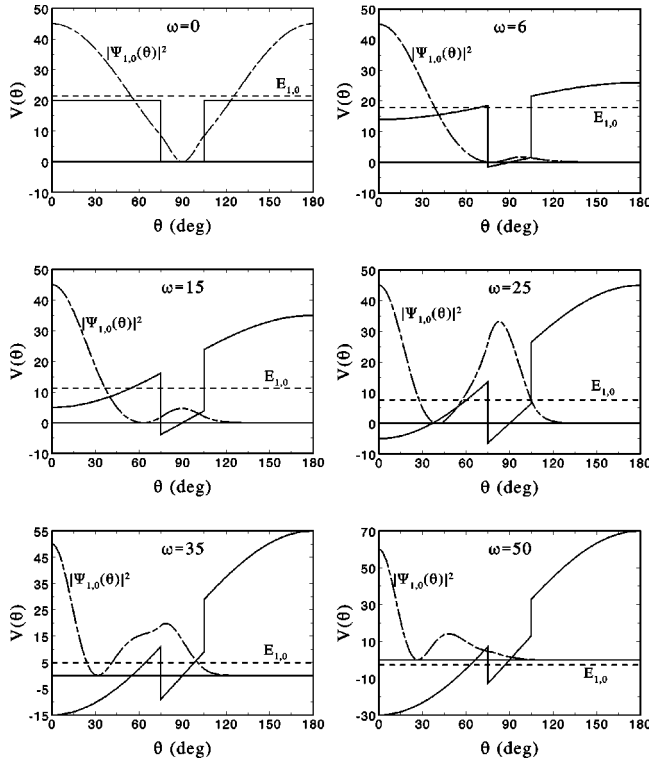


FIG. 8. Potential energy $V(\theta) = V^{\text{hin}}(\theta) - \omega \cos \theta$ and angular distribution of molecular wave function $|\Psi_{1,0}(\theta)|^2$ for a horizontally adsorbed molecule as functions of θ for different electric field strengths. $V^{\text{hin}}(\theta)$ is the horizontal-conical-well hindrance potential with $V_0 = 20$, $\alpha = 75^\circ$, and $\beta = 180^\circ - \alpha$.

dominant. Therefore, the variations of energy are similar to those of free dipole molecule in an external electric field.

C. Rotational-state distributions

The measurement of final rotational-state distributions of molecules desorbing from a surface is one of the familiar experimental methods to study rotational motion of adsorbed molecules. To compare with the experimental data, we employ the sudden unhindrance approximation to calculate the final rotational-state distributions as proposed in the works of Gadzuk and his co-workers.⁴⁻⁶ We assumed that the desorption is induced by a fast process, i.e., the hindering potential is suddenly switched off and, thus, the pure hindered-to-free rotational transition takes place without changing the wave function. If the external electric field persists during the desorption process, the free-rotational states of a desorbing dipole molecule in an electric field can be expressed in terms of spherical harmonics:²⁶

$$\Psi_m^{\text{free}}(\theta, \phi) = \sum_{j'=m}^{\infty} c_{j',m} Y_{j',m}(\theta, \phi). \quad (18)$$

The probability of ending up in the J th free-rotational state is the sum of rotational Franck-Condon factors between the final state $\Psi_{J,m}^{\text{free}}$ and the hindered-rotational state $\Psi_{L,m'}^{\text{hin}}$, weighted by appropriate thermal factors; that is,

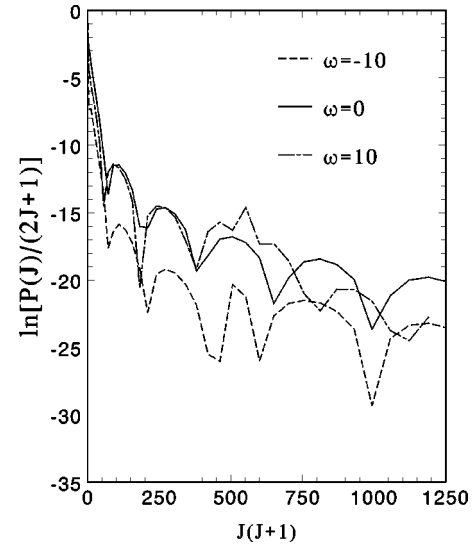


FIG. 9. Rotational-state distributions of suddenly desorbing molecule for various field strength parameters. In the calculation, we set $B/k_B T = 1$ and the molecule was assumed vertically adsorbed with hindrance parameters $V_0 = 20$ and $\alpha = 30^\circ$.

$$P(J) = \frac{1}{Z_{\text{hin}}} \sum_{m,L,m'} \exp(-E_{L,m'}/k_B T) |\langle \Psi_{J,m}^{\text{free}} | \Psi_{L,m'}^{\text{hin}} \rangle|^2, \quad (19)$$

where T is the surface temperature, k_B is the Boltzmann constant, and Z_{hin} is the partition function of the hindered rotor.

Figure 9 shows the calculated rotational-state distributions based on Eq. (19) for various field strength parameters. In the calculation, we set $B/k_B T = 1$, and the molecule was assumed vertically adsorbed with hindrance parameters $V_0 = 20$ and $\alpha = 30^\circ$. In Fig. 9, the curves are plotted in the form $\ln[P(J)/(2J+1)]$ vs $J(J+1)$. It is known that for a Boltzmann distribution a straight line with slope $= -B/k_B T$ should be obtained. From Fig. 9 one can see that the non-Boltzmann feature and oscillatory structure with alternate drops and plateaus of the rotational-state distributions still display when an external electrical field is present. However, the positions of the dips and the maxima are displaced.

To apply our calculation to a more realistic system, let us consider the Cs-CN adsorption system. Figure 10 shows the calculated rotational distribution for CN* desorbing from Cs surface based on Eq. (19) for various field strength parameters. The measured distribution for Cs-CN adsorption system in the absence of electric field³ is presented for comparison. In our calculation, the hindering potential was modeled as a vertical conical well with cone opening angle $\alpha = 11.36^\circ$ and potential barrier height $V_0 = 10\,030$ (i.e., $V_0 \approx 2.45$ eV). These hindrance parameters for Cs-CN adsorption system have been determined in our previous work.¹⁰ Since the electric field strength parameters we used in the calculation are much less than the potential barrier height V_0 , the electronic wave functions of the adsorbed molecule on a surface in the presence of an external electrical field are expected to undergo a mild variation during the desorption

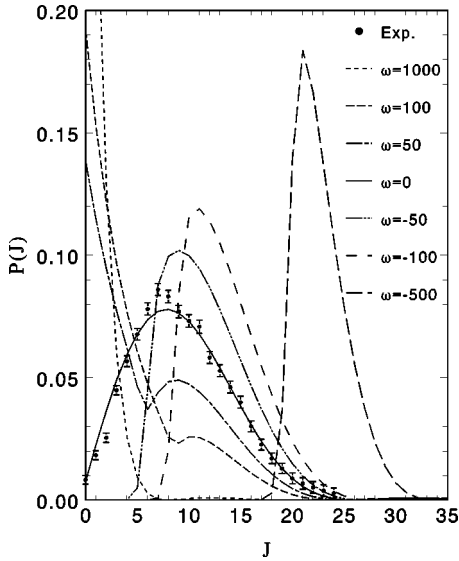


FIG. 10. Rotational-state distribution for CN* desorbing from Cs surface for various field strength parameters. In the calculation, the molecule was assumed vertically adsorbed with hindrance parameters $V_0=10\,030$ and $\alpha=11.36^\circ$.

process. Furthermore, the bond length and dipole moment of adsorbed molecule can be assumed not to be affected.

Figure 10 shows that the rotational-state distributions are significantly influenced by the external electric field. One can note that, for the $\omega < 0$ case, when the field strength is increased, the distribution shifts towards the high- J region. However, for the $\omega > 0$ case, the distribution shifts towards the low- J region as the field strength is increased. The shift of rotational-state distribution with electric field can be realized by the fact that, at low enough temperature, the final free-state distribution is mainly due to the conversion of initial ground-hindered-rotational-state energy. For the case of $\omega < 0$, as we gradually increase the electric field strength, the energy of ground-hindered-rotational state starts to increase because ω is still much less than V_0 (see Fig. 3), and thus the overlaps of ground-hindered-rotational state with high- J free-rotational states become more prominent. This causes the distribution to shift towards the high- J region. However, for the $\omega > 0$ case, as the field strength is increased, the energy of ground-hindered-rotational state starts to decrease (see Fig. 2), and the overlaps of ground-hindered-rotational state with low- J free-rotational states become more prominent. Therefore, the distribution shifts towards the low- J region.

Finally, an additional remark on the finite-conical-well model is made. Certainly, using a simplified analytical po-

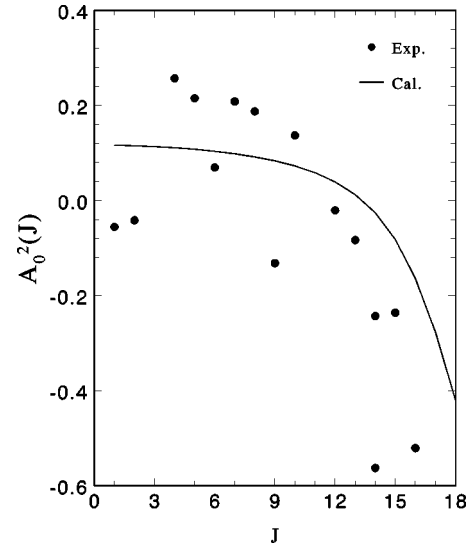


FIG. 11. Quadrupole moments for the desorption of CO from $\text{Cr}_2\text{O}_3(0001)$ as a function of quantum number J . Filled circles: experimental data points.

tential is not state of the art. Molecule-surface interaction potentials can nowadays be mapped out in great detail by *ab initio* electronic structure methods. However, as we have seen in our previous⁸⁻¹⁰ and present works, the simplified model shows interesting results. Furthermore, qualitative concepts and mechanisms can also be derived from the investigations. For example, we can justify our model by the performance of calculations on the rotational alignment of the desorbing molecules.

When a molecule desorbs from a solid surface,^{11-14,16,18} the quadrupole moment $A_0^2(J)$ is a measure of the rotational alignment and is defined as $A_0^2(J) = \langle J | (3J_z^2 - J^2) / J^2 | J \rangle$.³⁴ In the classical limit, the value of $A_0^2(J)$ represents the ensemble average of $(3 \cos^2\chi - 1)$ where χ is the angle between the angular momentum vector \mathbf{J} of the molecule and the surface normal. The value of $A_0^2(J)$ ranges from $+2$ to -1 , where positive values present helicopterlike motion (\mathbf{J} vector prefers to parallel to the surface normal), negative values correspond cartwheel-like motion (\mathbf{J} vector prefers to perpendicular to the surface normal).

To compare with the possible observed data, we calculate the quadrupole moment $A_0^2(J)$ by the results obtained in our model of finite conical well. According to the sudden unhindrance approximation, the quadrupole moment of the alignment distribution can be evaluated by the following equation:

$$A_0^2(J) = \frac{\sum_{m,L,m'} \exp(-E_{L,m'}/k_B T) \langle Y_{J,m} | \frac{3J_z^2 - J^2}{J^2} | Y_{J,m} \rangle \langle Y_{J,m} | \Psi_{L,m'}^{\text{hin}} \rangle^2}{\sum_{m,L,m'} \exp(-E_{L,m'}/k_B T) |\langle Y_{J,m} | \Psi_{L,m'}^{\text{hin}} \rangle|^2}. \quad (20)$$

Figure 11 shows our calculated results compared with the experimental results of the rotational alignment in the pho-
todesorption of CO from $\text{Cr}_2\text{O}_3(0001)$.^{16,18} The hindrance
parameters we used here are $V_0=2000$ and $\alpha=120^\circ$.

It was observed experimentally the quadrupole moment of
desorbing CO changes its sign from positive to negative with
increasing rotational quantum number J . Theoretically we
could reproduce a positive quadrupole moment for small
quantum number J and thus corresponds to the helicopterlike
desorbing, while a negative quadrupole moment of desorbing
CO can be obtained and thus corresponds to the cartwheel-
like desorbing for larger quantum number J . This result
agrees qualitatively with the experimental observations as
can be noted from Fig. 11.

To see more profoundly that our calculated results can
yield positive values of quadrupole momentum for small an-
gular momentum and negative values for large J states, we
examine the expectation value $\langle Y_{J,m} | (3\mathbf{J}_z^2 - \mathbf{J}^2) / \mathbf{J}^2 | Y_{J,m} \rangle$ in
Eq. (20). For a specific quantum number J , this expectation
value is positive for high $|m|$ values and is negative for low
 $|m|$ values. In the summation of Eq. (20), only the low-lying
hindered-rotational states $\Psi_{L,m'}^{\text{hin}}$ dominate due to the thermal
factor. We calculated the overlapping factors $|\langle Y_{J,m} | \Psi_{L,m'}^{\text{hin}} \rangle|^2$
between the free-rotational states $Y_{J,m}$ and the low-lying
hindered-rotational states $\Psi_{L,m'}^{\text{hin}}$. Our results showed that,
when J is small, the calculated value of $|\langle Y_{J,m} | \Psi_{L,m'}^{\text{hin}} \rangle|^2$ for
a specific L is larger for $\Psi_{L,m'}^{\text{hin}}$ states with larger $|m|$, which
correspond to more horizontally distributed wave functions.
This makes the hindered molecule pernt to the helicopterlike
desorption and yield a positive quadrupole moment. On the
contrary, when J is larger, the low-lying $\Psi_{L,m'}^{\text{hin}}$ states corre-
spond smaller $|m|$ and then negative expectation values
 $\langle Y_{J,m} | (3\mathbf{J}_z^2 - \mathbf{J}^2) / \mathbf{J}^2 | Y_{J,m} \rangle$. Our results also showed that,
when J is larger, the calculated value of $|\langle Y_{J,m} | \Psi_{L,m'}^{\text{hin}} \rangle|^2$ for
a specific L is larger for $\Psi_{L,m'}^{\text{hin}}$ states with smaller $|m|$, which
correspond to more vertically distributed wave functions.
This makes the hindered molecule tend to the cartwheel-like
desorption in larger J states and yield a negative quadrupole
moment.

IV. CONCLUSIONS

We have investigated the electric field effect of adsorbed
dipole molecules. The surface hindering potential to which
the adsorbed molecule is subjected was modeled as a finite
conical well and an dipole-field interaction was added to the
hindering potential. The molecular wave functions were ex-

pressed in terms of the eigenfunctions of adsorbed molecule
in the free field situation.

Our results show that for the vertically adsorbed dipole
molecules, if the external electric field orients the molecular
axis toward molecular preferred orientation, the ground-state
energy decreases as the electric field is increased, while the
excited-state energies increase to a maximum and then de-
crease as the field is increased. While, if the external electric
field orients the molecular axis against molecular preferred
orientation, there are avoided crossings of two energy levels
as the field is increased and finally all state energies decrease
rapidly as the field strength is strong enough. On the other
hand, for the horizontally adsorbed molecules, there are
smoother avoided crossings of two adjacent levels as the
field strength is increased and finally all state energies de-
crease rapidly for very strong field. The avoided crossing of
two adjacent energy levels is due to the redistribution of
wave function between different potential well regions.

By employing the sudden unhindrance approximation, the
rotational-state distributions of molecules desorbing from a
solid surface in the presence of external electric field were
calculated. When the calculated distributions were plotted
semilogarithmically, the non-Boltzmann feature and oscilla-
tory structure with alternate drops and plateaus of distribu-
tions displayed. We applied our calculation to more realistic
Cs-CN adsorption system. Our results showed that the
rotational-state distributions are significantly influenced by
the external electric field. When the electric field is applied
to orient the molecular axis against the molecular preferred
orientation, the distribution shifts towards the high- J region,
since the electric field increases the ground-state energy of
adsorbed molecule. However, when the electric field is ap-
plied to orient the molecular axis towards the molecular pre-
ferred orientation, the distribution shifts towards the low- J
region, since the electric field decreases the ground-state en-
ergy of adsorbed molecule.

We have calculated the rotational alignment in the pho-
todesorption of CO from $\text{Cr}_2\text{O}_3(0001)$ by the solutions to the
finite conical well. Our calculated results showed that at low- J
values the CO molecules desorb like a helicopter, while
at high J values a cartwheel-like motion is preferred. This
result is in qualitative agreement with the experimental
observation.

ACKNOWLEDGMENTS

This work was supported by the National Science Coun-
cil, Taiwan, Republic of China under the Grants Nos. NSC
91-2112-M-018-014 and NSC 91-2120-M-009-002.

*Author to whom correspondence should be addressed. Electronic
mail: ytshih@cc.ncue.edu.tw

†Electronic mail: dschuu@cc.nctu.edu.tw

¹A.W. Kley, A.C. Luntz, and D.J. Auerbach, Phys. Rev. Lett. **47**,
1169 (1981).

²R.R. Cavanagh and D.S. King, Phys. Rev. Lett. **47**, 1829 (1981).

³J. Xu, A. Barnes, R. Albridge, C. Ewig, N. Tolk, and L.D. Hulett,
Jr., Phys. Rev. B **48**, 8222 (1993).

⁴J.W. Gadzuk, U. Landman, E.J. Kuster, C.L. Cleveland, and R.N.
Barnett, Phys. Rev. Lett. **49**, 426 (1982).

⁵U. Landman, Isr. J. Chem. **22**, 239 (1982).

⁶J.W. Gadzuk, U. Landman, E.J. Kuster, C.L. Cleveland, and R.N.
Barnett, J. Electron Spectrosc. Relat. Phenom. **30**, 103 (1983).

⁷U. Landman, G.G. Kleiman, C.L. Cleveland, E. Kuster, R.N. Bar-
nett, and J.W. Gadzuk, Phys. Rev. B **29**, 4313 (1984).

⁸Y.T. Shih, D.S. Chuu, and W.N. Mei, Phys. Rev. B **51**, 14 626

- (1995).
- ⁹Y.T. Shih, D.S. Chuu, and W.N. Mei, *Solid State Commun.* **99**, 819 (1996).
- ¹⁰Y.T. Shih, D.S. Chuu, and W.N. Mei, *Phys. Rev. B* **54**, 10 938 (1996).
- ¹¹D.C. Jacobs, K.W. Kolasinski, R.J. Madix, and R.N. Zare, *J. Chem. Phys.* **87**, 5038 (1987).
- ¹²H. Hou, S.J. Gulding, C.T. Rettner, A.M. Wodtke, and D.J. Auerbach, *Science* **277**, 80 (1997).
- ¹³D. Wetzig, R. Dopheide, M. Rutkowski, R. David, and H. Zacharias, *Phys. Rev. Lett.* **76**, 463 (1996).
- ¹⁴M. Rutkowski, D. Wetzig, and H. Zacharias, *Phys. Rev. Lett.* **87**, 246101 (2001).
- ¹⁵A. Eichler, J. Hafner, A. Groß, and M. Scheffler, *Chem. Phys. Lett.* **311**, 1 (1999).
- ¹⁶I. Beauport, K. Al-Shamery, and H.-J. Freund, *Chem. Phys. Lett.* **256**, 641 (1996).
- ¹⁷S. Thiel, M. Pykavy, T. Klüner, H.-J. Freund, R. Kosloff, and V. Staemmler, *Phys. Rev. Lett.* **87**, 077601 (2001).
- ¹⁸S. Thiel, M. Pykavy, T. Klüner, H.-J. Freund, R. Kosloff, and V. Staemmler, *J. Chem. Phys.* **116**, 762 (2002).
- ¹⁹R. Schinke, *J. Chem. Phys.* **76**, 2352 (1982).
- ²⁰E.W. Müller, *Z. Physik* **A 106**, 541 (1937).
- ²¹E.W. Müller, *Z. Physik* **131**, 136 (1951).
- ²²R. Gomer, *Surf. Sci.* **299/300**, 129 (1994).
- ²³T.T. Tsong, *Surf. Sci.* **299/300**, 153 (1994).
- ²⁴H. J. Kreuzer, in *Chemistry and Physics of Solid Surfaces*, edited by R. Vanselow and R. Howe (Springer-Verlag, New York, 1990), Vol. VIII.
- ²⁵G. Herzberg, *Molecular Spectra and Molecular Structure. I. Spectra of Diatomic Molecules*, 2nd ed. (Van Nostrand, New York, 1950).
- ²⁶K. von Meyenn, *Z. Phys. A* **231**, 154 (1970).
- ²⁷R.P. Pan, R.D. Etters, K. Kobashi, and V. Chandrasekharan, *J. Chem. Phys.* **77**, 1035 (1982).
- ²⁸J.W. Riehl and C.J. Fisher, *J. Chem. Phys.* **59**, 4336 (1973).
- ²⁹V.M. Allen and P.D. Pacey, *Surf. Sci.* **177**, 36 (1986).
- ³⁰*Handbook of Mathematical Functions*, edited by M. Abramowitz and I. A. Stegun (Dover, New York, 1970).
- ³¹L. D. Landau and E. M. Lifshitz, *Quantum Mechanics*, 3rd ed. (Pergamon, New York, 1977).
- ³²G. Bastard, E.E. Mendez, L.L. Chang, and L. Esaki, *Phys. Rev. B* **28**, 3241 (1983).
- ³³D. Ahn and S.L. Chuang, *Appl. Phys. Lett.* **49**, 1450 (1986).
- ³⁴C.H. Greene and R.N. Zare, *J. Chem. Phys.* **78**, 6741 (1983).